Molecular Dynamics Simulation Studies of a Model System for Liquid Crystals Consisting of Rodlike Molecules in NPT Ensemble

Chang Jun Lee, Hoon Goo Sim, Woon Chun Kim, Song Hi Lee,† and Hyungsuk Pak*

Department of Chemistry, Seoul National University, Seoul 151-742, Korea
†Department of Chemistry, Kyungsung University, Pusan 608-736, Korea
Received December 7, 1999

Molecular dynamics simulation studies for thermotropic liquid crystalline systems composed of rodlike molecules with 6 Lennard-Jones interaction sites were performed in NPT ensemble. Within the range of temperature studied, the system exhibited isotropic and smectic phase. For the characterization of the smectic phase, we examined the structure of the liquid crystalline phase *via* the radial distribution function, its longitudinal and transverse components to the director, and other orientational correlation functions. In the smectic A phase, our results showed a large anisotropy in translational motion (*i.e.*, $D_{\perp} >> D_{\parallel}$), and the decay of the collective orientational correlation function of rank two became slower than that of the single particle orientational correlation function of rank one. Comments on the spontaneous growth of orientational order directly from the isotropic phase are given.

Introduction

Liquid crystals, so called mesophase, are fascinating states of matter, which have long been investigated for their rich and diverse physical properties and delicate phase transition behavior.[1-4] These materials have become of interest in a variety of applications, mainly due to their large optical anisotropy which can be easily manipulated by applied fields and surface interactions.[5] For example, twist nematic (TN) devices have proved phenomenally useful, and their response to applied fields and surface interactions is well understood.

The thermotropic liquid crystals concerned in this research exhibit three different mesophases –nematic, smectic and cholesteric (chiral nematic)– which are clearly distinguished from a normal (isotropic) liquid and a crystal. The liquid crystalline behavior may be affected by molecular properties such as molecular shape, flexibility of the chemical bonds, charge distribution, and polarizability.[6] There have been a number of recent computer simulation studies, which have attempted to model liquid crystal molecules by the use of atomistic potentials with an all-atom representation for liquid crystalline materials of low molecular mass.[7-12] But the high costs of these simulations render the systematic investigation of the state function of such realistic model systems unfeasible. In practice, studies of realistic potentials have been limited to a few hundred picoseconds: long enough to equilibrate the internal molecular structure, but too short to observe the spontaneous formation of ordered phases from an isotropic fluid. Hence, less complex molecular models have been used in Molecular Dynamics (MD) and Monte Carlo (MC) simulations to elucidate the phase behavior of liquid crystals by taking into account some of the above-mentioned molecular properties.

A range of computer simulations (MC, MD) using simple models have been investigated. Hard nonspherical models have demonstrated the importance of excluded volume effects in promoting liquid crystalline behavior. Simulations of hard ellipsoids have shown the presence of nematic (N_+),[13] discotic nematic (N_-)[14] and biaxial nematic phases,[15] while studies of hard spherocylinders have also shown the presence of smectic[13,16] phases. Many studies have been made that include the anisotropic attractive interaction as well as the anisotropic repulsive interaction arising from the molecular shapes. Using the Gay-Berne potential,[17] a variety of liquid crystalline phases have been investigated.[18-20] The Gay-Berne potential is an interaction applied to the centers of mass of the molecules, with parameters depending on the mutual orientation of the molecules as well as their separation, and it is essentially Lennard-Jones in character. Its main drawback lies in the fact that it is not transferable, that is, it cannot be used to construct the interactions of molecule viewed as an assembly of atoms.[21]

In the present work, we choose a simple approach: calamitic mesogenic (mesophase-producing) compounds that consist of long, narrow, lath-like and fairly rigid molecules, are modeled as a set of linear rigid rod molecules interacting*via* a Lennard-Jones potential. This approach is straightforward and naturally considers the anisotropic repulsive and attractive interaction between mesogens. We present here the results of the isothermal-isobaric (NPT) molecular dynamics simulation for this model, which show the isotropic-smectic phase transition and the characteristic dynamic behavior in each phase.

The organization of this paper is as follows: In the next section, we describe a molecular model and molecular dynamics simulation techniques employed here to study the phase behavior. Section III is devoted to the main results of our simulation, followed by the concluding remarks.

Molecular Model and Simulation Methods

Recently, the phase behavior of a system of hard spherocylinders for liquid crystal was re-investigated by McGrother *et al.*[16(a)] with the isothermal-isobaric Monte Carlo simula-

tion technique. For sufficiently large aspect ratios (cylinder length(L)/diameter(D)), the system exhibited various phases: isotropic, nematic, smectic A and solid phase. Especially, there was a transition directly from the isotropic to the smectic A phase for the system with an aspect ratio of L/D = 3.2. Is it possible to show similar phase behavior by considering the anisotropic attractive and repulsive interaction? In this paper, our main concern is not to elucidate the full phase diagram, but to show the characteristic phase behavior including the dynamics by using a simple model. So we have confined our consideration to a model molecule with a certain geometry (see below).

For a full discussion on our model and the details of the simulation method, we refer to our previous paper[22] and references therein. As in our previous work, the calamitic liquid crystal molecule is modeled as a rigid rod with 6 equally spaced interaction sites. The intermolecular potential is given by the sum of site-site atomic potentials for which we employ the Lennard-Jones (LJ) 12-6 potential. In this work, all the interaction sites are considered to be equivalent and we adopt the second parameter set, that is, the length parameter σ of LJ potential reduced by 2/3 with the unchanged energy parameter ε of Jorgensen *et al.*'s.[23] In summary, the molecular parameter is as follows: according to the definitions adopted in the hard spherocylinder (HSC) model, the length of molecule is 7.02 Å, the aspect ratio is about 2.7 (smaller than 3), σ is 2.615 Å, and ε is about 0.5986 kJ/mol.

The initial system has 256 molecules inside a cubic box with a density of 0.81 g/cm^3. The initial orientations of all the molecules are chosen as parallel to the z-axis of the simulation box. The positions of the center of mass of the molecules are distributed at random in such a way that the distances between the interaction sites at different molecules are greater than 0.9σ.

An accompanying consideration in the study of phase transition is the change in density, entropy, and free energy. In this study, we have chosen the NPT molecular dynamics simulation method devised by Evans *et al.*[24(a),24(b)] to monitor the change in density or the volume of the system. A detailed description of the derivation of the equations of motion for constraint method was given in our previous paper and references.[24] Special care in using the boundary condition and considerations on the long-range correction were also described in our previous work. Gear's fifth-order predictor-corrector algorithm[24,25] was used for time integration of the equations of motion for translation and rotation with a time step of 2 fs(10^{-15}s). The radius of spherical cut-off was chosen as one-half box. The temperature range in this study is 200.0 K-298.15 K, and the pressure is 1 atm.

During the simulations, orientational and translational orderings of the rodlike molecules were monitored; the former *via* the calculation of the orientational order parameter[26(a)] S_2 and the latter *via* the radial distribution function $g(r)$. The orientational order parameter, S_2, is given by

$$S_2 = \frac{1}{N}\sum_{i=1}^{N} P_2(\cos\theta_i). \tag{1}$$

Here, N is the number of molecules, P_2 is the *second*-rank Legendre polynomial (*i.e.*, $P_2(\cos\theta_i)=(3\cos^2\theta_i-1)/2$), and θ_i is the angle between the symmetry axis ($\mathbf{u}_i$) of molecule i and the director ($\mathbf{n}$) describing the average direction of alignment for the molecules. Since the direction of $\mathbf{n}$ is not known *a priori*, the order parameter has to be determined using another approach. In the present work, S_2 is associated with the largest eigenvalue obtained through the diagonalization of the ordering tensor[26(b)]

$$Q_{\alpha\beta} = \frac{1}{N}\sum_{i=1}^{N}\left(\frac{3}{2}u_{i\alpha}u_{i\beta}-\frac{1}{2}\delta_{\alpha\beta}\right), \quad (\alpha, \beta=x, y, z), \tag{2}$$

where $u_{i\alpha}$ is the α-component of the orientational unit vector of molecule i, and $\delta_{\alpha\beta}$ is the Kronecker δ-symbol. The eigenvector associated with the largest eigenvalue provides the director $\mathbf{n}$. The value of S_2 in the isotropic phase will be close to 0, while it will tend to 1 in a highly ordered phase.

The radial distribution function[24(c)] of the center of mass of the molecules is defined by

$$g(r) = \frac{V}{N^2}\langle\sum_{i=1}^{N}\sum_{j\neq i}^{N}\delta(\mathbf{r}-\mathbf{r}_{ij})\rangle. \tag{3}$$

Here, $\mathbf{r}_{ij}$ is the vector between the centers of mass of the molecules i and j, and V is the volume of the system. Two components $g_{\parallel}(r)$ and $g_{\perp}(r)$ of $g(r)$ were used to monitor the translational order parallel and perpendicular to the director, respectively.

It was observed that the direction of $\boldsymbol{n}$ varies quite slowly during the course of the simulation at equilibrium state. Consequently, a new director was evaluated for each set of coordinate data used in the compilation of $g(r)$, $g_{\parallel}(r)$ and $g_{\perp}(r)$.

The dynamic behavior of molecules is analyzed in terms of the time correlation function defined by

$$C_A(t) = \frac{\langle A(t_0)A(t+t_0)\rangle}{\langle A(t_0)A(t_0)\rangle}, \tag{4}$$

where $A(t)$ is the classical dynamic property of a molecule evaluated at time t. To study the reorientational motion, we calculate the single-particle reorientational correlation functions[27] defined by

$$C_l^s(t) = \frac{\langle P_l(\boldsymbol{u}_i(t_0)\cdot\boldsymbol{u}_i(t+t_0))\rangle}{\langle P_l(\boldsymbol{u}_i(t_0)\cdot\boldsymbol{u}_i(t_0))\rangle}, \quad (l=1, 2) \tag{5}$$

and the analogous collective quantity:

$$C_2^c(t) = \frac{\sum_{j\neq i}\langle P_2(\boldsymbol{u}_i(t_0)\cdot\boldsymbol{u}_j(t+t_0))\rangle}{\sum_{j\neq i}\langle P_2(\boldsymbol{u}_i(t_0)\cdot\boldsymbol{u}_j(t_0))\rangle}. \tag{6}$$

In the above equations, the angular brackets imply an average over particles as well as over the time origins.

Results and Discussion

In Table 1, we summarize our simulation results for the average Lennard-Jones energy (E_{LJ}) per particle, density (ρ),

Table 1. Summary of simulation data. Figures in parentheses are estimated (one standard deviation) errors in the last quoted digits

T (K)	Equilibration Time (ps)	Production Time (ps)	E_{LJ} (kJ/mol)	ρ (g/cm^3)	S_2
298.15	200	200	-15.6(8)	1.02(6)	0.08(3)
270.0	200	200	-18.7(5)	1.21(3)	0.08(3)
240.0	200	200	-22.3(5)	1.38(3)	0.13(4)
220.0	300	300	-31.9(3)	1.74(1)	0.70(1)
200.0	300	300	-33.3(3)	1.81(9)	0.67(1)

and order parameter (S_2) at equilibrium state. Within the range of our simulation, the solid phase was not reached.

A break in the density and order parameters between 240.0 K and 220.0 K implies the phase transition from a disordered isotropic liquid to an ordered liquid crystalline phase. Though we consider the temperature difference, the density change ($\Delta\rho/\rho \approx 0.26$) between 240.0 K and 220.0 K is very large compared with that of isotopic-nematic transition characterized as weak first order. For example, in the case of *para*-azoxy-anisole(4,4′-dimethoxyazoxybenzene, PAA), one of the well-known nematogens, the value of $\Delta\rho/\rho$ is about 0.0035 (see Table on page 224 of ref. 3 and cited original references therein). The above observations imply that this phase transition may be a first-order phase transition. It may be proper to say that the precise characterization of this phase transition requires the monitoring of the change in Gibbs free energy, enthalpy, entropy, and density at transition temperature.

The ordering of molecules into layers is most clearly seen through the behavior of the functions $g(r)$, $g_{\parallel}(r)$ and $g_{\perp}(r)$ shown in Figure 1. In the isotropic phase, small peaks in $g(r)$ indicate some correlations between neighboring sites. By reducing the temperature in the isotropic phase, the growth of peaks can be detected along with the deepening of the trough, which is accompanied by an increase in the resolution of peaks at higher distances. At T=220.0 K, $g(r)$ takes on the appearance of a well ordered system with a substantial first solvation peak and other peaks over one-half size of the simulation box. The feature of the liquid crystalline phase is provided by the parallel and perpendicular components $g_{\parallel}(r)$, $g_{\perp}(r)$. The smectic phase is characterized more unambiguously by the clear periodic density wave shown in $g_{\parallel}(r)$, the projection of the pair correlation function along the director, corresponding to the smectic layering (see Figure 1(c)). The isotropic phase does not exhibit this behavior, as shown in Figure 1(a) and (b). $g_{\parallel}(r)$ at T=220.0 K indicates smectic layers with a layer spacing of approximately 9.0 Å, which is larger than the length of the rigid molecule, 7.02 Å. The perpendicular component, $g_{\perp}(r)$, can be used to monitor the intra-layer order. Over the length scale studied here, $g_{\perp}(r)$ at T=220.0 K implies that short-range positional order exists within the layer.

Orientational order is also shown in the behavior of the orientational pair correlation functions $g_n(r)$,[27]

$$g_n(r) = g_{n0n}(r) / g_{000}(r) = \langle P_n(\cos\theta_{ij}(r))\rangle \quad (n = 2, 4, 6) \quad (7)$$

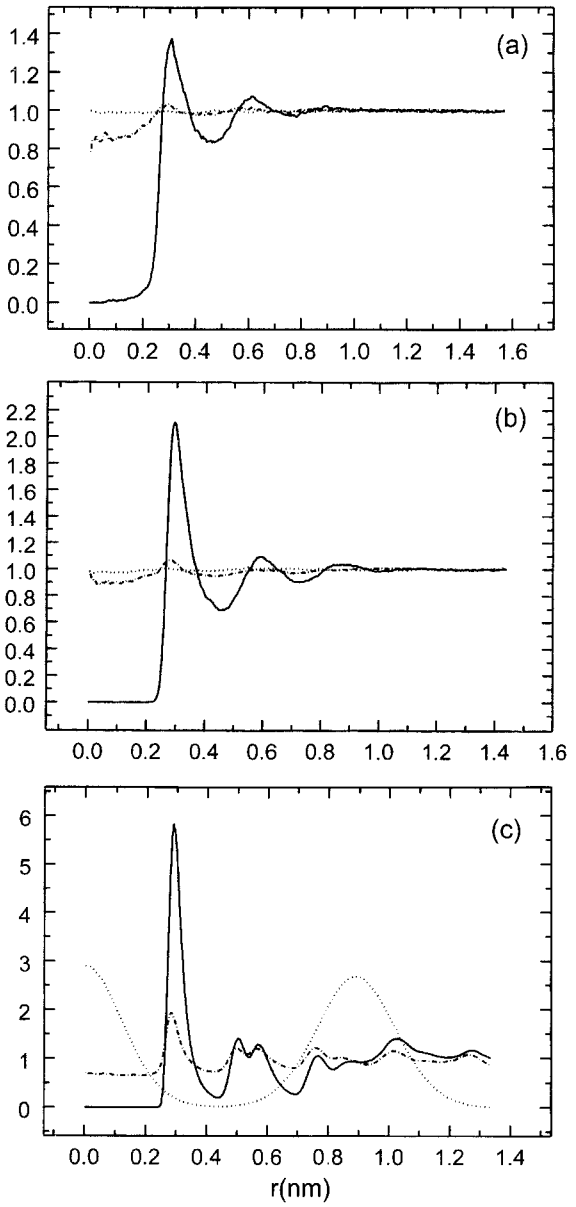

Figure 1. Radial distribution functions for center of mass of rigic molecules: $g(r)$ (solid line (—)), $g_{\parallel}(r)$ (dotted line (····)), $g_{\perp}(r)$ (dotdashed line (-·--)) (a) T=298.15 K, (b) T=240.0 K, (c) T= 220.0 K.

where $\theta_{ij}(=\cos^{-1}(\boldsymbol{u}_i\cdot\boldsymbol{u}_j))$ is the angle between molecular axes $\boldsymbol{u}_i$ and $\boldsymbol{u}_j$ of moleucles i and j, a distance r apart, $P_4(\cos\theta_{ij})=(35\cos^4\theta_{ij} - 30\cos^2\theta_{ij} + 3)/8$, and $P_6(\cos\theta_{ij}) = (231\cos^6\theta_{ij} - 315\cos^4\theta_{ij} + 105\cos^2\theta_{ij} - 5)/16$. These functions provide a measure of the decay of the angular correlations with the radial distance, and thus can be used to quantify the orientational order of the phase. In the isotropic phase, these functions decay to zero at large r, but in the orientationally ordered phase, they go to limiting values at larger r, which is clearly shown in Figure 2.

Snapshots of equilibrated configurations at T=220.0 K and T=200.0 K (not shown here), combined with data analysis of the translational ordering, indicate that the orientationally ordered phase is a smectic phase (see Figure 6). To

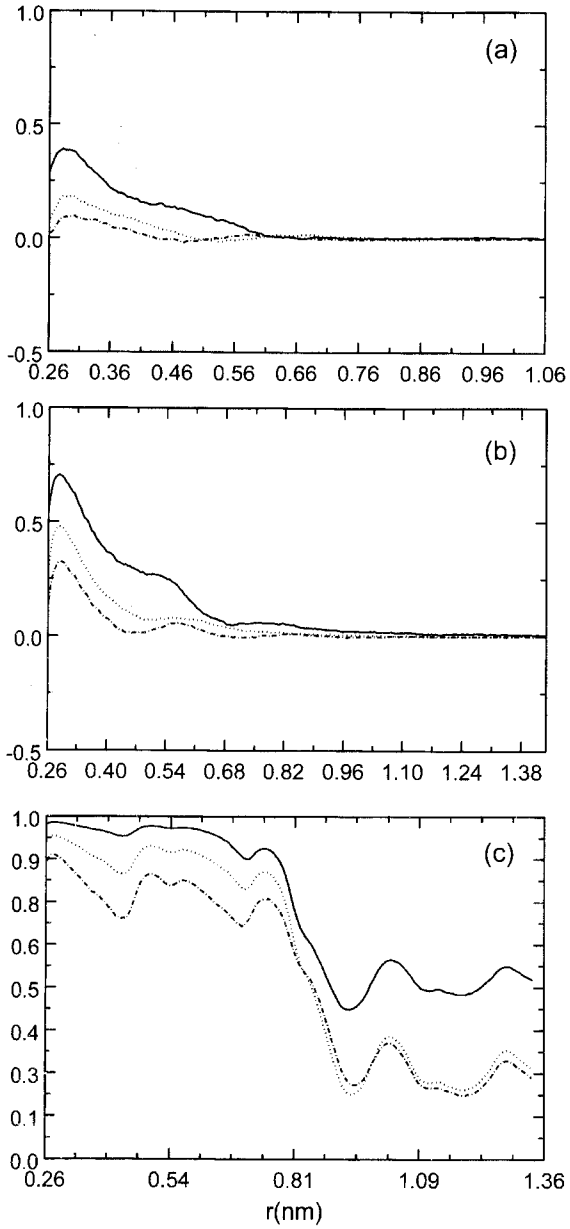

Figure 2. Orientational pair correlation functions $g_n(r)$: $g_2(r)$ (solid line (—), $g_4(r)$ (dotted line (····)), $g_6(r)$ (dotdashed line (-·-·)) (a) T=298.15 K, (b) T=240.0 K, (c) T=220.0 K.

exclude a possible artifact caused by finite system size, we carried out other simulations for the same system composed of 96 and 512 molecules. From these surveys, we concluded that the liquid crystalline phase is a smectic A phase (S_A).

We now discuss the results for the dynamics of the system. The anisotropic translational self-diffusion in ordered media can be described by a *second*-rank tensor. In uniaxial liquid crystals this tensor is diagonal and axially symmetric with principal values $D_{\parallel}$ (the diffusion constant parallel to the director) and $D_{\perp}$ (the diffusion constant perpendicular to the director). The self-diffusion constants were evaluated from the slope at long times of the mean-square displacement using the Einstein relation[24(c)]

Table 2. Diffusion constants obtained from the simulation at various temperatures

T (K)	D ($10^{-9}m^2/s$)	$D_{\parallel}$ ($10^{-9}m^2/s$)	$D_{\perp}$ ($10^{-9}m^2/s$)	$D_{\parallel}/D_{\perp}$
298.15	9.58	10.1	9.33	1.08
270.0	6.75	6.78	6.74	1.01
240.0	3.42	3.46	3.40	1.02
220.0	0.955	4.67×10^{-2}	1.41	3.31×10^{-2}
200.0	0.212	7.82×10^{-3}	0.314	2.49×10^{-2}

$$D = \lim_{t\to\infty} \langle (\Delta \boldsymbol{r}(t))^2 \rangle / 6t, \quad (\Delta \boldsymbol{r}(t) = \boldsymbol{r}(t+t_0) - \boldsymbol{r}(t_0)),$$

$$D_n = \lim_{t\to\infty} \langle (\Delta \boldsymbol{r}(t) \cdot \boldsymbol{n})^2 \rangle / 2t, \tag{8}$$

where $\Delta \boldsymbol{r}(t)$ is the displacement vector of center of mass of a

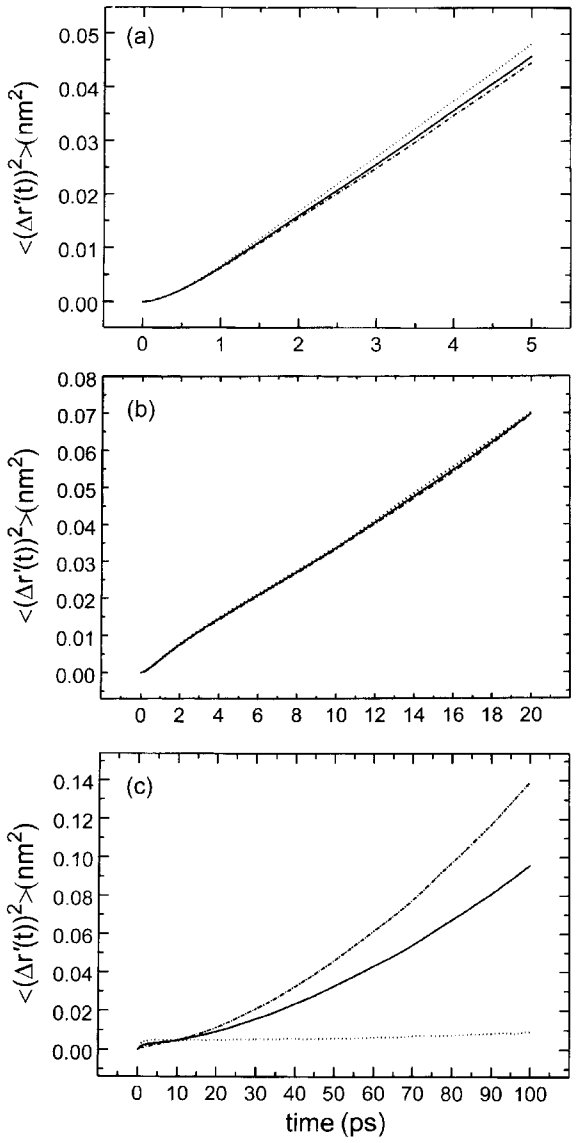

Figure 3. Mean square displacement and its components versus time: $\langle(\Delta r(t))^2/6\rangle$ (solid line (—), $\langle(\Delta r_{\parallel}(t))^2/2\rangle$ (dotted line (····)), $\langle(\Delta r_{\perp}(t))^2/2\rangle$ (dotdashed line (-·-·)) (a) T=298.15 K, (b) T=240.0 K, (c) T=220.0 K.

molecule during a time t, $\boldsymbol{n}$ is a unit vector parallel or perpendicular to the director at $t = t_0$, and the angular brackets < > indicate an average over all molecules as well as over time origins.

In Table 2, we summarize the results of our simulation. The characteristic behavior of the diffusive motion in the isotropic phase and smectic phase is exhibited in Figure 3. In Figure 3(a) and (b), we can see a ballistic feature due to inertial behavior at very short time regimes and well-known diffusive behavior after short times in the isotropic phase. (Note that the mean square displacement curves in this figure are prescribed to include the dividing numerical factor 2 or 6) The diffusion of the rigid molecules in the smectic A phase at short times is solid-like, that is, the molecules can move rapidly within a restricted region and then diffuse much slowly in a liquid-like manner after longer times (see Figure 3(c)). Experimental measurements of smectic phases show Arrhenius-type behavior of $D_{\parallel}$ and $D_{\perp}$ with strongly different activation energies, namely $E_{\parallel} > E_{\perp}$ due to the layering structure. Consequently, with decreasing temperature the anisotropy ratio ($D_{\perp}/D_{\parallel}$) can change from < 1 to >> 1.[28] In our simulation, the anisotropy ratio ($D_{\perp}/D_{\parallel}$) in smectic A phase exceeds 1 as shown in Table 2.

The behavior of the molecular reorientation in the isotropic and smectic phase can be seen in Figure 4. The short-time behavior of the orientational time correlation functions in the isotropic phase exhibit characteristic features of inertial components, which is shown in Figure 4(a). From Figure

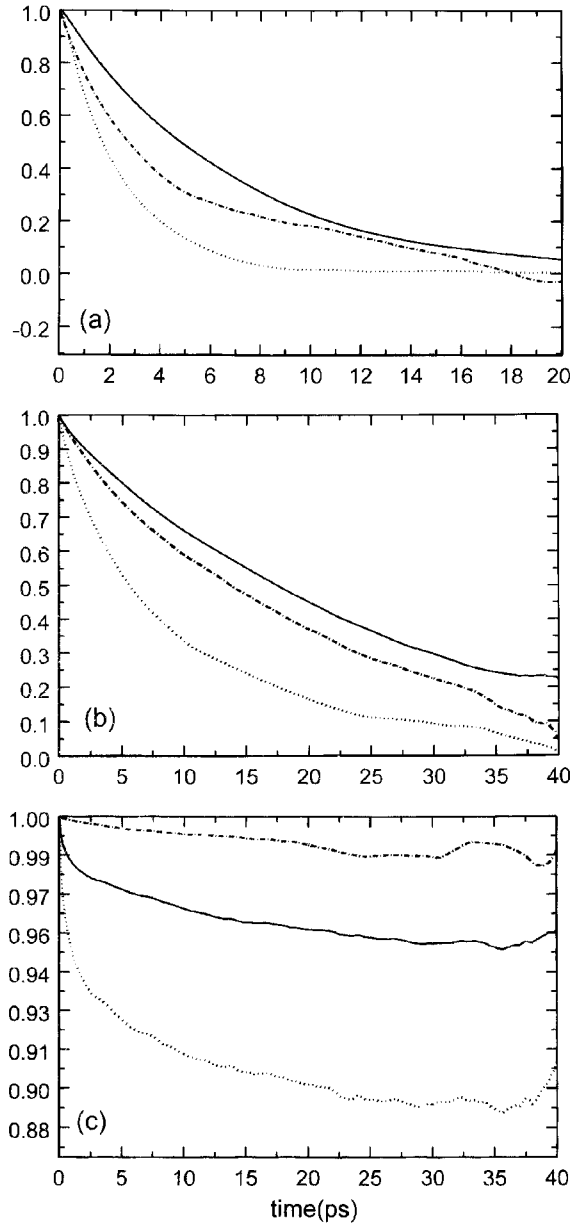

Figure 4. Reorientational time correlation functions versus time single-particle correlation functions of rank one $C_1^s(t)$ (solid line (—)), rank two $C_1^s(t)$ (dotted line (····)), and collective particle correlation function of rank two $C_1^s(t)$ (dot-dashed line (----)) (a) T=298.15 K, (b) T=240.0 K, (c) T=220.0 K.

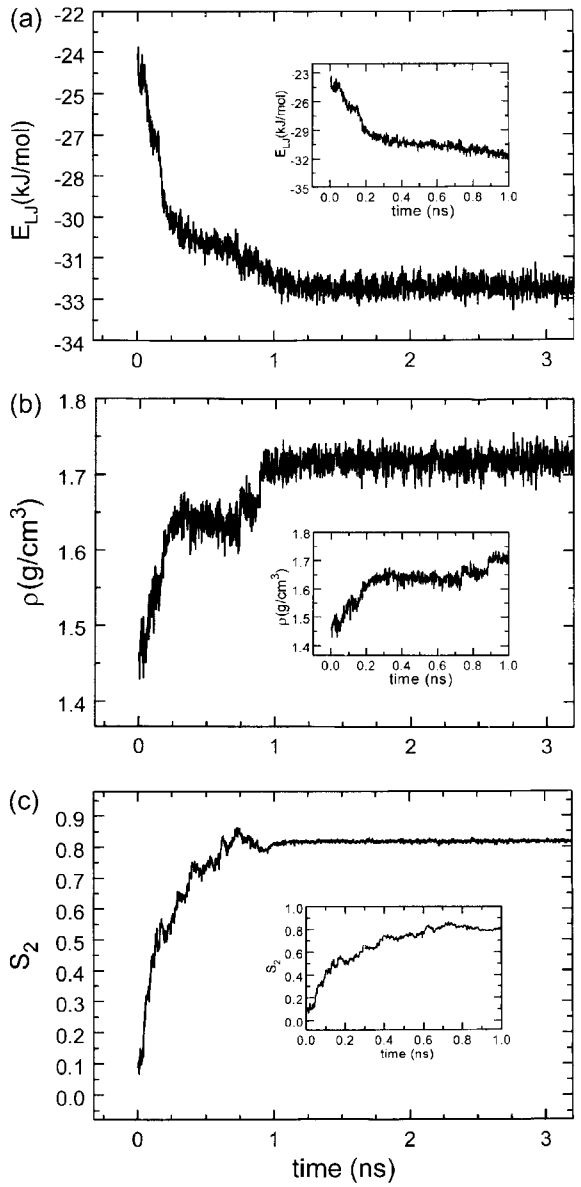

Figure 5. The evolution of some physical quantities from isotropic state during 3.2 ns at T=220.0 K and 1 atm (a) E_{LJ} per particle (b) density (ρ) (c) order parameter (S_2). The inlets in each figure show more clearly the process to reach the stable state.

4(a) and 4(b), we can find that correlation time of the molecular reorientation in the isotropic phase increases as the temperature falls. Figure 4(c) shows three distinct features: (i) The orientational correlation functions exhibit a drastic slowing down at the smectic phase. (ii) $C_2^c(t)$ decays even slower than $C_1^s(t)$, which implies an increase in the collective orienational correlation in the smectic phase and the coupling of collective motion with single molecular motion. (iii) The time correlation functions do not show a single exponential decay at long time, which suggests the complex nature of the orientational motion in the smectic region.

Before closing this section, we will address our results for the spontaneous growth of orientational order from the isotropic phase to the smectic phase. One phase point taken at T=240.0 K in its equilibrium state was quenched to 220.0 K. Figure 5 shows the evolutions of E_{LJ} per particle, density and S_2 from the isotropic fluid phase to an ordered phase during 3.2 ns. Our observations can be summarized as follows:

(i) The molecules tend to align along the longest axis of the simulation box, that is, the director and smectic layers align along the body-diagonal of the cubic simulation box.

(ii) Though there is some discrepancy in the order parameter (S_2) between the two states which started from different initial configurations (see Table 1 and Figure 5), the main feature of the smectic A phase that develops is clearly retained.

(iii) The lower S_2 value at T=220.0 K in Table 1 compared with this experiment and the reduction of S_2 at T=200.0 K, imply that the size of the cubic box was not properly devised for the smectic ordering. This prediction was confirmed by our later experiment for 512 molecules under the same conditions.

(iv) The evolution time from isotropic phase to smectic phase is relatively short compared with experiment and other simulations.[12,29] This may be due to the simple nature of our model, differences in initial value of S_2 and method of simulation.

(v) No clear evidence for pretransion behavior in orientational motion from isotropic to smectic phase was found over the evolution period.

(vi) Some of the molecules are lying between the smectic layer over the time region studied here, which prevents the perfect smectic ordering (see Figure 6(d)).

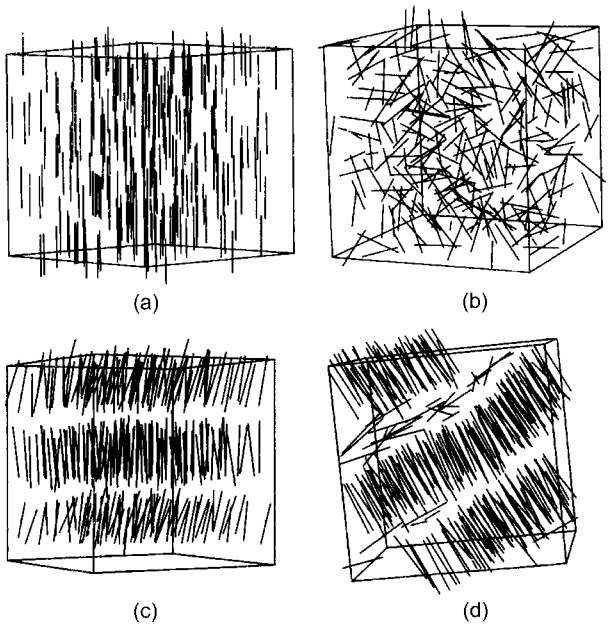

Figure 6. Snapshots showing the orientational order of (a) initia stage, (b) equilibrium state at T=240.0 K (isotropic phase), (c equilibrium state at T=220.0 K (smectic phase), (d) the state at tim t=3.2 ns starting from an isotropic phase with S_2=0.1.

Concluding Remarks

Over the last decades, computer simulations have brought considerable progress in our understanding of the behavior of liquid crystals. Achievements in the experimental area and the diverse field of liquid crystal research have given us more challenging problems.

In this paper, we have presented the results of a molecular dynamics simulation of model system for liquid crystal in the NPT ensemble. To consider the two possible origins, anisotropic repulsive and attractive interactions, for forming the liquid crystalline phase, we used the usual Lennard-Jones potential. The characteristic structural feature of calamiticliquid crystal was modeled as a rigid rod. The rodlike molecules comprising 6 equally-spaced Lennard-Jones interaction sites exhibited isotropic, smectic A phase within the temperature range studied.

For the proper assignment of the liquid crystalline phase, we analyzed the positional and orientational structures: the former through the radial distribution function, with components parallel and perpendicular to the director, and the latter through order parameter and orientational correlation functions. The liquid crystalline nature of a given material is most easily established by the anisotropy of the physical properties such as refractive index, dielectric permittivity and transport properties. This macroscopic anisotropy implies that the molecular anisotropy related any of these properties does not average out to zero as is the case in an isotropic phase. In our simulation, smectic A phase exhibits a significant anisotropy in translational motion ($D_\perp >> D_\parallel$). The decays of the orientational correlation functions are gradually reduced with the lowering the temperature in the isotropic phase. In the smectic phase, the decay of the collective orientational function becomes even slower than the single particle orientational correlation function of rank one, which also slows down conspicuously.

Our observations for the spontaneous growth of the orientational order from isotropic phase to smectic A phase imply that system size should be devised with great care for smectic ordering. The possible effect caused by the use of cubic boundary condition with the isotropic variation of box size for isotropic-smectic phase transition in NPT ensemble should be thoroughly investigated.

Acknowledgment. The present studies were supported (in part) by the Basic Science Research Institute Program, Ministry of Education, 1998, Project No. BSRI-98-3414.

References

1. de Gennes, P. G.; Prost, J. *The Physics of Liquid Crystals*; Clarendon Press: Oxford, U. K., 1994.
2. Chandrasekhar, S. *Liquid Crystals*; Cambridge University Press: Cambridge, U. K., 1977.
3. *The Molecular Physics of Liquid Crystals*; Luckhurst, G. R., Gray, G. W., Eds.; Academic Press: New York, U. S. A., 1979.
4. *Handbook of Liquid Crystals*; Demus, D., Goodby, J., Gray, G. W., Spiess, H. -W., Vill, V., Eds.; Wiely-VCH: New York, U. S. A., 1998; Vol. 1. *Fundamentals*.
5. (a) Sage, I. C. In *Handbook of Liquid Crystals*; Demus, D., Goodby, J., Gray, G. W., Spiess, H. -W., Vill, V., Eds.; Wiely-VCH: New York, U. S. A., 1998; Vol. 1. *Fundamentals*, p 731. (b) Collings, P. J.; Hird, M. *Introduction to Liquid Crystals: Chemistry and Physics*; Taylor and Francis: Bristol, U. S. A., 1997; p 271.
6. Gray, G. W. In *The Molecular Physics of Liquid Crystals*; Luckhurst, G. R., Gray, G. W., Eds.; Academic Press: New York, U. S. A., 1979; chapter 1 and 12.
7. Huth, J.; Mosell, T.; Nicklas, K.; Sariban, A.; Brickmann, J. *J. Phys. Chem.* **1994**, *98*, 7685.
8. Komolkin, A. V.; Laaksonen, A.; Maliniak, A. *J. Chem. Phys.* **1994**, *101*, 4103.
9. Cross, C. W.; Fung, B. M. *J. Chem. Phys.* **1994**, *101*, 6839.
10. Hauptmann, S.; Mosell, T.; Reiling, S.; Brickmann, J. *Chem. Phys.* **1996**, *208*, 57.
11. Sandström, D.; Komolkin, A. V.; Maliniak, A. *J. Chem. Phys.* **1997**, *106*, 7438.
12. McBride, C.; Wilson, M. R.; Howard, J. K. *Mol. Phys.* **1998**, *93*, 955.
13. (a) *For a review of hard convex body fluids see* Allen, M. P.; Evans, G. T.; Frenkel, D.; Mulder, B. M. In *Advances in Chemical Physics*; Prigogine, I., Rice, S. A., Eds.; John Wiley & Sons, Inc: New York, U. S. A., 1993; Vol. LXXXVI. p 1. (b) Frenkel, D.; Mulder, B. M.; McTague, J. P. *Phys. Rev. Lett.* **1984**, *52*, 287.
14. Frenkel, D.; Eppenga, R. *Phys. Rev. Lett.* **1982**, *49*, 1089.
15. Camp, P. J.; Allen, M. P. *J. Chem. Phys.* **1997**, *106*, 6681.
16. (a) McGrother, S. C.; Williamson, D. C.; Jackson, G. *J. Chem. Phys.* **1996**, *104*, 6755. (b) Bolhuis, P.; Frenkel, D. *J. Chem. Phys.* **1997**, *106*, 666.
17. (a) Gay, J. G.; Berne, B. J. *J. Chem. Phys.* **1981**, *74*, 3316. (b) Clever, D. J.; Care, C. M.; Allen, M. P.; Neal, M. P. *Phys. Rev. E* **1996**, *54*, 559.
18. de Miguel, E.; Rull, L. F.; Chalam, M. K.; Gubbins, K. E. *Mol. Phys.* **1991**, *74*, 405.
19. Brown, J. T.; Allen, M. P.; del Río, E. M.; de Miguel, E. *Phys. Rev. E* **1998**, *57*, 6685.
20. Ravichandran, S.; Perera, A.; Moreau, M.; Bagchi, B. *J. Chem. Phys.* **1998**, *109*, 7349.
21. Paolini, G. V.; Ciccotti, G.; Ferrario, M.; *Mol. Phys.* **1993**, *80*, 297.
22. Lee, S. H.; Kim, H. S.; Pak, H. *J. Chem. Phys.* **1992**, *97*, 6933.
23. Jorgensen, W. L.; Briggs, J. M.; Conteras, M. L. *J. Chem. Phys.* **1990**, *94*, 1683.
24. (a) Evans, D. J.; Morris, G. P. *Chem. Phys.* **1983**, *77*, 63. (b) Evans, D. J.; Morris, G. P. *Comput. Phys. Rep.* **1984**, *1*, 297. (c) Allen, M. P.; Tildesley, D. J. *Computer Simulation of Liquids*; Clarendon Press: New York, U. S. A., 1987, *For a discussion of constraint methods, see* p 234 and *for a Gear's predictor-corrector algorithm, see* p 340.
25. Gear, C. W. *Numerical Initial Value Problems in Ordinary Differential Equations*; Prentice-Hall: New Jersey, U. S. A., 1971.
26. (a) Zannoni, C. In *The Molecular Physics of Liquid Crystals*; Luckhurst, G. R., Gray, G. W., Eds.; Academic Press: New York, U. S. A., 1979, p 51. (b) Penna, G. L.; Catalano, D.; Veracini, C. A. *J. Chem. Phys.* **1996**, *105*, 7097.
27. Allen, M. P.; Frenkel, D. *Phys. Rev. Lett.* **1987**, *58*, 1748.
28. (a) Noack, F. In *Handbook of Liquid Crystals*; Demus, D., Goodby, J., Gray, G. W., Spiess, H. -W., Vill, V., Eds.; Wiely-VCH: New York, U. S. A., 1998; Vol. 1. *Fundamentals*, p 581. (b) Krüger, G. H. *Phys. Rep.* **1982**, *82*, 229.
29. (a) Wilson, M. R. *J. Chem. Phys.* **1997**, *107*, 8654. (b) McBride, C.; Wilson, M. R. *Mol. Phys.* **1999**, *97*, 511.